U N I V E R S I T É P A R I S - S U D

Institut National de Physique Nucléaire et de Physique des Particules

U.E.R.

du

LABORATOIRE

de

L'ACCÉLÉRATEUR LINÉAIRE

TRANSITION AND SYNCHROTRON RADIATION PRODUCED
BY ELECTRONS AND PARTICLE DISCRIMINATION

by

B. JEREMIE, J-P. REFFILLY, G. SAUVAGE,
M. ECOFFET*, J.C. CHOLLET, M. STALINAS,
J-M. GAILLARD, A. HRISCHU and Ph. JEAN.

* University of Geneva - (Switzerland)

FR7701225
LAL 1202
July 1976

TRANSITION AND SYNCHROTRON RADIATION PRODUCED BY ELECTRONS AND PARTICLE DISCRIMINATION

ABSTRACT

Transition radiation from a radiator of 650 lithium foils has been studied in a MWPC filled with a Xenon-CO_2 mixture for two experimental configurations. With the chamber immediately after the radiator, particle discrimination comparable to those reported in the litterature (90% efficiency for electrons, 10% for hadrons) have been observed. With magnetic bending between the radiator and the Xenon chamber typical efficiencies of 87% for electrons and less than 0.4% for hadrons have been measured. The discrimination obtained is at least a factor 20 better than for the more conventional configuration. In the latter case, synchrotron radiation has also been observed.

RESUME

Nous avons mesuré le rayonnement de transition produit par un radiateur de 650 feuilles de lithium pour deux configurations expérimentales différentes. Le détecteur utilisé était une chambre à fils proportionnelle remplie d'un mélange de Xénon et de CO_2. Avec la chambre placée immédiatement après le radiateur, nous avons obtenu des facteurs de discriminations du particule comparables à ceux rapportés dans la littérature (soit une efficacité de 90% aux électrons et une efficacité de 10% aux hadrons). Avec un aimant déflecteur placé entre le radiateur et la chambre à Xénon, nous avons mesuré des efficacités de 87% aux électrons et inférieures à 0,4% aux hadrons. Le facteur de discrimination ainsi obtenu est au moins 20 fois meilleur qu'avec la configuration expérimentale habituellement utilisée. Nous avons aussi observé le rayonnement synchrotron produit dans l'aimant déflecteur.

1. INTRODUCTION

Transition radiation [1] has been used in several test experiments to separate electrons from other particles. Recently Fischer et al.[2] have shown that with a radiator made of lithium foils the effective number of photons can be very much increased. In other experiments where mylar foils had been used [3], the self absorption of the X rays limited the number of foils to about 100 per module. With the low Z of lithium the self absorption is greatly reduced and radiators with about 1000 foils can be used.

We have tested a 650 lithium foil radiator constructed for the SPS experiment on hyperon leptonic decays [4] in a test beam at the CERN proton synchrotron. Since in the set up planned for the SPS experiment the X-ray detector, a MWPC Xenon chamber can be placed either immediately after the radiator or separated from it by the spectrometer magnet, we have done the test for both configurations, using a standard 2m magnet to simulate the effect of the spectrometer magnet. The insertion of a magnetic bending between the radiator and the X-ray detector brings the obvious advantage of a spatial separation between the dE/dx energy loss of the particle and the energy deposited by the transition radiation X rays and it should widely improve the discrimination between electrons and other particles.

2. EXPERIMENTAL SET UP

The test has been performed in a beam which could be tuned to give electrons and (or) hadrons from 1.6 GeV/c to 12.9 GeV/c. The two experimental configurations are shown in Fig.1a corresponding to the radiator against the xenon chamber and Fig.1b with the magnet in between the radiator and the chamber. In both cases, high precision beam chambers [5] determine the direction of the incoming particle to an accuracy of ± 0.4 mrad in each projection. They are also used to eliminate multiparticle events. The trigger was given by a coincidence between several scintillation counters : A, B and C for the first experimental configuration (Fig.1a) ; A, B, C and D for the second case (Fig.1b). To identify the particles in the beam a Čerenkov counter and a block of lead glass have been used. From the lead glass pulse height distribution, we estimate that the hadron contamination

in the electron samples is less than 0.5% at all energies. The electron contamination in the hadron samples is about 0.1%.

The radiator is made of 650 lithium foils, about 50 μm thick separated by intervals of 320 μm, corresponding to 2% of radiation length and to a physical length of 25 cm. It has an active area of 56 x 56 cm² and has been built at CERN by assembling lithium bricks of 50 foils 4.4 cm wide and 60 cm long. To minimize the inefficiency due to cracks between adjacent bricks, every layer is displaced laterally by two millimeters with respect to the previous one. The aluminium container is closed at both ends by two mylar windows of 100 μm and 50 μm. A circulation of dry helium is maintained in the container and between the windows.

The detector is a multiwire proportional chamber with two 5 mm gaps. The two HT planes and the readout plane are made of 20 μm golden tungsten vertical wires with pitches of 1 mm and 4 mm for the HT and readout planes respectively. To minimize the X ray absorption before the first HT plane the 50 μm mylar entrance window is at a distance of 0.6 mm from the HT plane. The chamber is evacuated, filled with a 80% Xe, 20% CO_2 mixture and sealed. The gap corresponds to a compromise between a good efficiency for X ray detection and a reasonable level of the ionization energy loss. With the chamber geometry and the gas mixture chosen, the charge collection time is 1 ns for ionizing particles. At the working voltage of 2 kvolts the chamber gain is 10^4. To obtain a linear signal information from the xenon chamber a charge amplifier with a FET input is used (Fig.2). The discharge time constant of the preamplifier is 22 μs and it can accept up to 10^6 pulses per second without saturation effect. The preamplifier is coupled through a 20 m coaxial cable to a single delay line clipping amplifier with a base line restorer. The clipping time is 250 ns and the output pulse is compatible with the Lecroy charge sensing ADC (model 2249A). In the case of an ionizing particle the output pulse is trapezoidal with a 150 ns rise and fall time and a 100 ns flat top. These are the minimum values compatible with the chamber geometry.

With standard X ray emitters, Fe^{55} (5.9 Kev), Nb^{93m} (16.6 Kev), Zn^{65} (8.0 Kev) and Cd^{109} (22.0 Kev), we have studied the linearity of the chamber response which is found to be better than ± 1%. During the test run the chamber energy resolution measured with 5.9 Kev X-rays from a Fe^{55} source was 40% (FWHM).

3. CONVENTIONAL DETECTION OF THE TRANSITION RADIATION

In the configuration of Fig.1a, eight wires had been equipped with amplifiers, covering a width of 3.2 cm slightly larger than the lateral dimension of the beam and the pulse heights were recorded into separate ADC channels.

Electrons were defined amongst the particles giving coincidences between the counters A, B, C by requiring a single track in the beam chambers a pulse from the Čerenkov counter and a large pulse height from the lead glass. For hadrons we required instead no pulse in the Čerenkov counter and a small pulse height from the lead glass.

From the position and the direction of the incoming particle in the beam chambers, the extrapolated position in the Xenon chamber is defined to a fraction of a millimeter. Since the transition radiation is emitted at very small angles, both the dE/dx of the particle and the transition X-rays are expected to register mostly only on the nominal wire nearest to the extrapolated position. With electrons we find that in 15% of the cases the energy is distributed over two wires or more because of the X-rays, whereas with hadrons we get only 2% of multiwire hits. For the analysis presented below we have summed the energies deposited over five wires, centered around the nominal wire. Fig.3 shows the spectra of the energy deposited in the xenon chamber for electrons and for hadrons of 6.5 Gev/c. In Fig.4 we have plotted the electron efficiency versus the hadron efficiency for four momenta. Above 5 Gev/c the hadrons are mostly protons, whereas for the lowest momentum of 2.6 Gev/c they are pions. In Table 1, we give as an example, the efficiencies obtained for electrons and for hadrons at the four momenta with a cut at 12 Kev on the energy released in the xenon chamber. The electron efficiency of 90% and the discrimination against hadrons by a factor 10 are comparable to previous results [5] obtained at CERN with a 700 foils lithium radiator.

4. BARE TRANSITION RADIATION

In the configuration of Fig.1b, a standard vacuum chamber with two 50 μm myler windows had been installed in the 2 m magnet between the radiator and the xenon chamber. It was filled with helium gas to minimize the X-ray

absorption. With a magnetic bending of 40 mrad, the particle trajectory and the expected impact of the transition radiation are separated by about 6 cm at the xenon chamber position. For that part of the test, sixteen wires had been equipped with amplifiers, four for dE/dx and twelve for transition radiation. These two regions were separated by seven wires (2.8cm). On line the trigger was given by a four fold coincidence ABCD (see Fig.1b). Off line a single track in the beam chambers and a hit in the dE/dx region of the xenon chamber have been required. In addition hadrons and electrons have been selected by using the Čerenkov and the lead glass information. Measurements have been done at five momenta from 1.6 Gev/c to 10.2 Gev/c.

For each particle the nominal wire in the transition radiation region is the closest to the extrapolation of the track measured with the beam chambers. Efficiencies for electrons and for hadrons, defined as the percentage of particles giving at least one hit on any of the five wires centered around the nominal wire, are given in Table 2 for the various momenta. The electron efficiency saturates at high momentum when the distance between the foils is smaller than the formation zone of the transition radiation. The raw numbers show that for all momenta the discrimination against hadrons is better than a factor of 150. The pulse width from the xenon chamber is 250 ns, much wider than the 50 ns gate applied to the beam chambers and a measurement at 6.5Gev/c has shown that 50% of the efficiency to hadrons is due to a spurious coincidence with an electron. A confirmation of this fact has been obtained by inserting a 1 mm copper plate after the radiator, which removes almost completely the transition radiation X rays. The hadron efficiency is then only 0.2%, to be compared to 0.4% without the plate. The remaining 0.2% are at least partly due to interactions of higher momentum hadrons, mostly in the lithium. Fig.5 shows the measured distribution of the energy released in the chamber by the transition radiation at 6.5 Gev/c. The mean energy is about 22 Kev and the average number of detected X-rays per electron is about 2 which explains why the electron efficiency is not unity.

With that configuration we have also measured the dE/dx distributions at 6.5 Gev/c for hadrons (mostly protons) and for electrons which are shown in Fig.6. Because of the relativistic rise the ionization energy loss is larger for electrons (6 Kev) than for hadrons (4 Kev). This difference helps in the first configuration to get a good efficiency for electrons without too much hadron contamination.

5. SYNCHROTRON RADIATION

In the configuration with magnetic bending, we have observed with electrons additional radiation spatially located in the xenon chamber between the regions where the ionization loss and the transition radiation w expected. This radiation is left intact when a 1 mm copper plate is inserted after the radiator, but before the magnet, whereas the transition radiation is suppressed. It disappears when the copper plate is inserted after the magnet in front of the xenon chamber . These observations suggest that the effect is due to synchrotron radiation. For a quantitative estimate we have limited our study to the three wires of the transition radiation region closest to the dE/dx region of the xenon chamber. We have considered only the electrons which, because of their position and direction in the beam chambers, could not send transition radiation X-rays on those wires. Due to the beam profile this corresponds to the majority of the electrons.

The magnetic deflection spanned by the three wires is 5.5 mrad. The number of photons [7] of energy ω to $\omega + d\omega$ emitted while the electron is deflected through an angle $\Delta\theta$ in the magnetic field is

$$n(\omega)\, d\omega\, \Delta\theta = \frac{\sqrt{3}}{2\pi}\, \alpha\, \gamma\, \Delta\theta\, \frac{1}{\omega_{cr}} \int_{\omega/\omega_{cr}}^{\infty} K_{5/3}(\eta)\, d\eta\, d\omega \qquad [1]$$

where the critical energy ω_{cr} is given by :

$$\omega_{cr} = \tfrac{3}{2}\, \gamma^3 \hbar\, c/\rho \qquad [2]$$

For our test the radius of curvature was 50 meters the same for all momenta corresponding to a critical energy of about 47 Kev at 10.2 Gev/c.

Taking into account the absorption and the detection efficiency as a function of the photon energy, we have computed the probability to observe at least one photon from synchrotron radiation in the specified region. Curve (A) of Fig.7 gives this efficiency as a function of the electron momentum for ρ = 50 m and $\Delta\theta$ = 5.5 mrad. The measured values also plotted in Fig. 7 exhibit the expected dependence with the momentum, but the yields are systematically lower than the curve by about 20%. This discrepancy reflects probably our limited knowledge of the absorption and of the detection efficiency over a wide range of photon energies. The satu-

ration of the calculated electron efficiency for high momento corresponds to the fact that, although more photons are emitted, their average energy being higher, the detection efficiency is lower. This situation can probably be improved with a different detector. The transition radiation spectrum discussed in the previous section contains a small contribution from the synchrotron radiation. The effect on the efficiency is at most 1% for the highest momentum.

During the test we have worked with a radius of curvature ρ = 50 m independent of the momentum chosen. For practical use we have also computed with Equation (1) the electron efficiency due to synchrotron radiation with a uniform field of 20 kgauss over a length Lo = 2 m. The absorption and the detection efficiency have the same dependence upon the photon energy as in the previous paragraph and the result is represented by the curve (B) of Fig. 7. For the same value of the field and a length L of the magnet, the efficiency scales as $(1 - e^{-\beta L})$. A change of the field value requires a new computation, but, as can be easily seen from Eq. (1), the efficiency increases with the field for a fixed magnet length. The shape of curve (B) depends strongly upon the detector. For instance with a chamber twice as thick the electron efficiency will still be about 80% at 50 Gev/c.

6. CONCLUSIONS

Transition radiation becomes a more powerful tool to discriminate between electrons and other particles when a magnet is inserted between the radiator and the X-ray detector. Because the magnetic bending separates spatially the impacts of the particle and of the transition radiation in the detector, discrimination factors of 200 or more are obtained. In an actual experiment additional background rejection may become possible with more detailed information from other parts of the set up. The electron efficiency is typically 87%. An important advantage is that the chamber gain is not anymore a critical parameter. The configuration with magnetic bending can be readily used in many experiments with spectrometer ; it will be in the hyperon SPS experiment.

Synchrotron radiation is also a significant means to select electrons in the same experimental configuration.

ACKNOWLEDGEMENTS

We are grateful to CERN for the permission to use the lithium laboratory for making the radiator and to K. LEY and G. MURATORI for their help. We have benefited from several fruitful consultations with C.W. FABJAN and W.J. WILLIS. We are deeply indebted to Ch.EECAN for the realisation of the amplifiers and we gratefully acknowledge the technical help of C. GUILLON.

	2.6 Gev/c	4.5 Gev/c	6,5 Gev/c	12,9 Gev/c
Electron efficiency	83.3 ± 0.6	89.3 ± 0.4	87.9 ± 0. 6	88.6 ± 0.6
Hadron efficiency	10.6 ± 0.2	9.3 ± 0.7	5.4 ± 0. 4	8.9 ± 0.4

TABLE I : Electron and hadron efficiencies in % for a 12 Kev cut
Results obtained with the conventional detector

	1.6 Gev/c	2.6 Gev/c	4.5 Gev/c	6.5 Gev/c	10.2 Gev/c
Electron efficiency	75.7 ± 1.4	84.4 ± 1.2	85.8 ± 0.9	86.5 ± 0.9	87.1 ±1.0
Hadron efficiency	0/208	0.28 ± 0.11	0.58± 0.23	0.45± 0.17	0.41±0.11

TABLE II : Electron and hadron efficiencies in % with magnetic bending.

REFERENCES

1. - V.L. GINZBURG and I.M. FRANK, JETP 16, 15 (1945)
G.M. GARIBYAN, JETP 10, 372 (1960)
M.L. TER. MIKAELYAN, Nuclear Physics 24, 43 (1961)
V.E. PAFOMOV, JETP 20, 353 (1965)
F.G. BASS and V.M. YAKOVENKO, Soviet Physics Uspekhi 8, 420 (1965).
(this paper contains an extensive bibliography).

2. - J. FISCHER, S. IWATA, V. RADEKA, C.L. WANG and W.J. WILLIS, Physics Letters 49B, 383 (1974)

3. - H. UTO, L.C.L. YUAN, G.F. DELL and C.L. WANG, Nuclear Instruments and Methods 97, 389 (1971)

4. - Charged Hyperon Proposal, CERN/SPSC/74-32, SPSC/P2 and addendum.

5. - B. MERKEL, Nuclear Instruments and Methods 94, 573 (1971)

6. - C.W. FABJAN and W.J. WILLIS, private communication.

7. - J. SCHWINGER, Physical Review 75, 1912 (1947).

FIGURE CAPTIONS

Fig. 1a : Plan view of the experimental set up without magnet

1b : Plan view of the experimental set up with magnet

Fig. 2 : Charge amplifier electronic diagram

Fig. 3 : Spectrum of the energy deposited in the xenon chamber by electrons and by hadrons of 6.5 Gev/c

Fig. 4 : Electron efficiency versus hadron efficiency at different momenta

Fig. 5 : Spectrum of the energy deposited in the xenon chamber by pure transition radiation for 6.5 Gev/c electrons.

Fig. 6 : dE/dx distributions at 6.5 Gev/c for hadrons and for electrons.

Fig. 7 : Synchrotron radiation. Expected and observed efficiencies as a function of the electron momentum.

Curve (A) with the left hand side scale corresponds to ρ = 50 m and $\Delta\theta$ = 5.5. mrad.

Curve (B) (right hand side scale) is obtained with a field of 20 kgauss over 2 m.

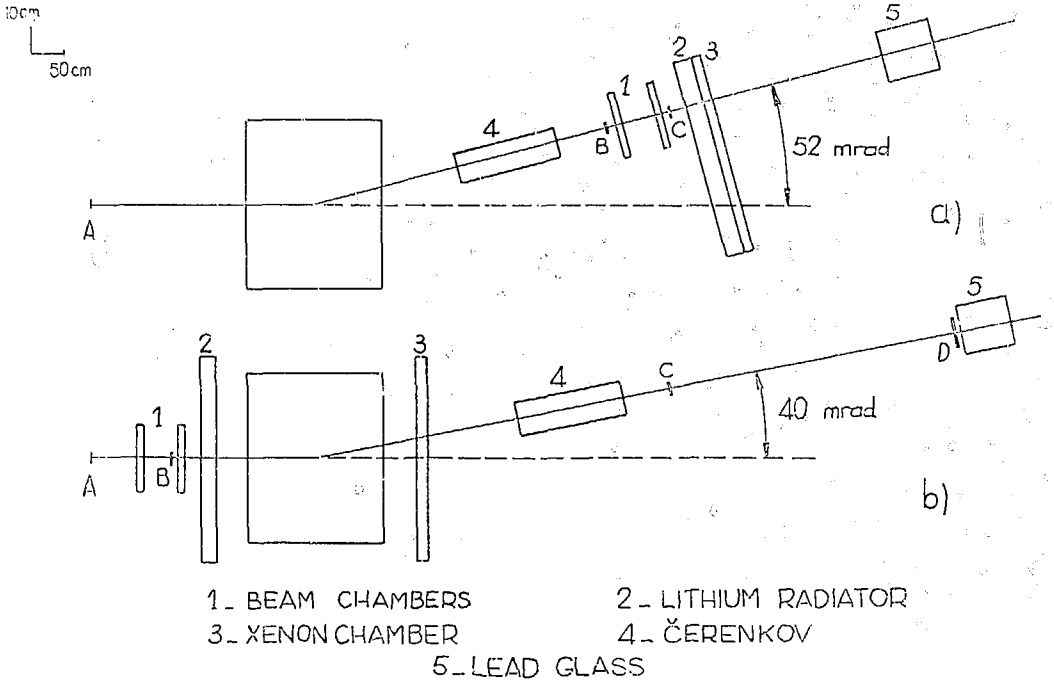

FIG.1 : a) PLAN VIEW OF THE EXPERIMENTAL SET UP WITHOUT MAGNET
b) PLAN VIEW OF THE EXPERIMENTAL SET UP WITH MAGNET

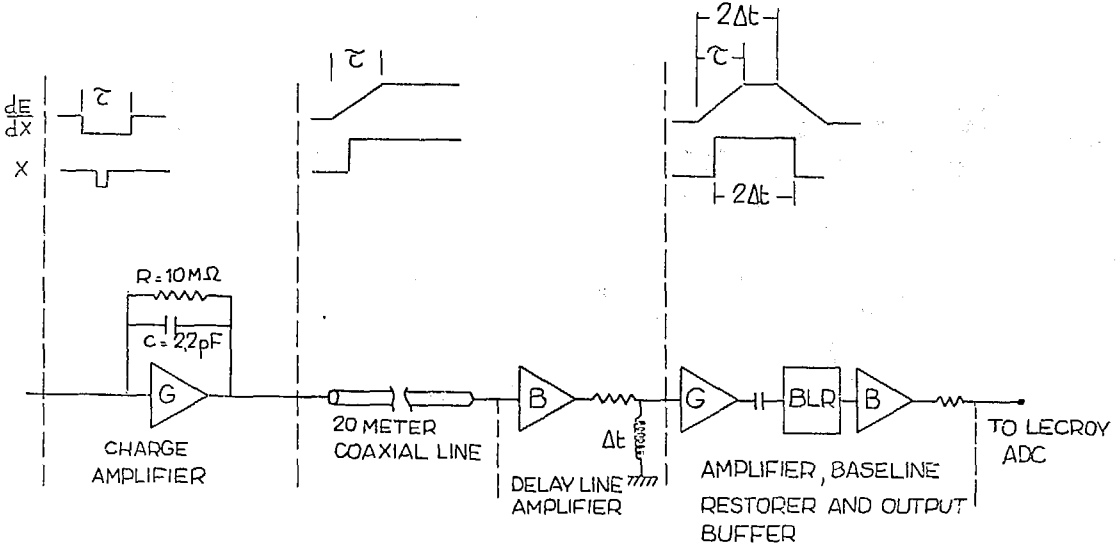

FIG.2 : CHARGE AMPLIFIER ELECTRONIC DIAGRAM

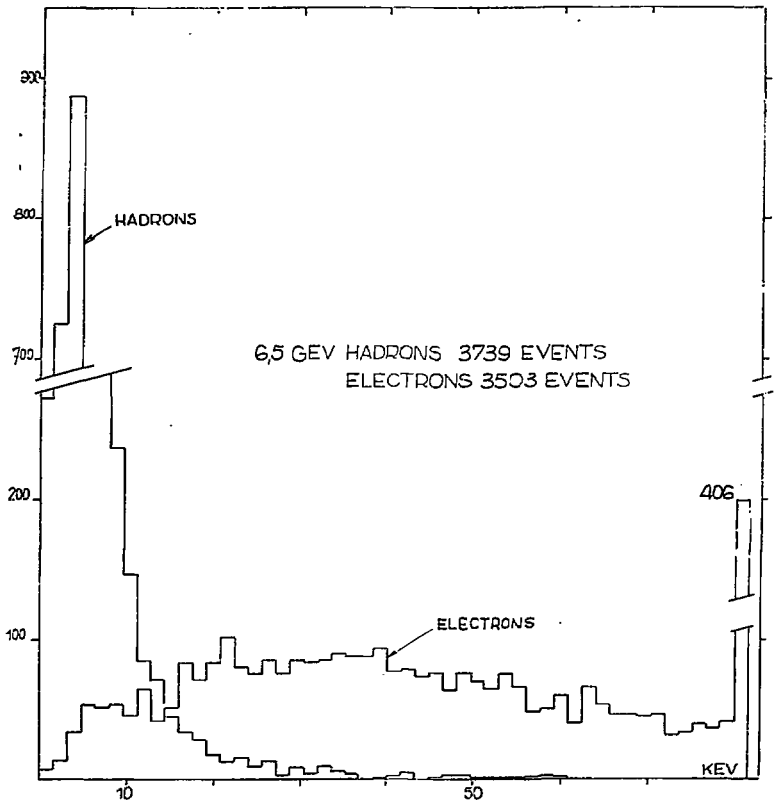

FIG.3 : SPECTRUM OF THE ENERGY DEPOSITED IN THE XENON CHAMBER BY ELECTRONS AND BY HADRONS OF 6.5 GeV/c.

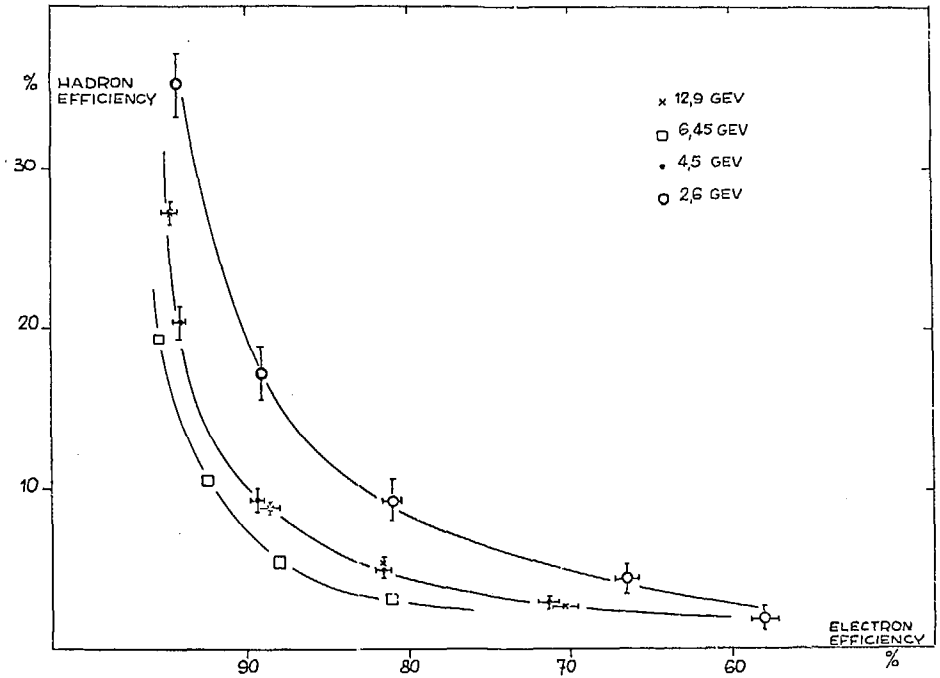

FIG.4 : ELECTRON EFFICIENCY VERSUS HADRON EFFICIENCY AT DIFFERENT MOMENTA

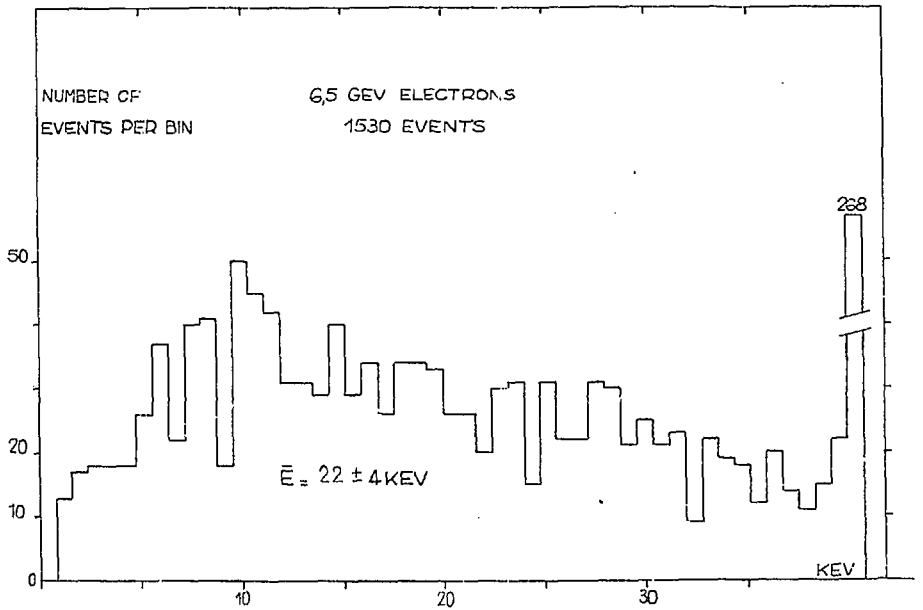

FIG.5 : SPECTRUM OF THE ENERGY DEPOSITED IN THE XENON CHAMBER BY PURE TRANSITION RADIATION FOR 6.5 GeV/c ELECTRONS.

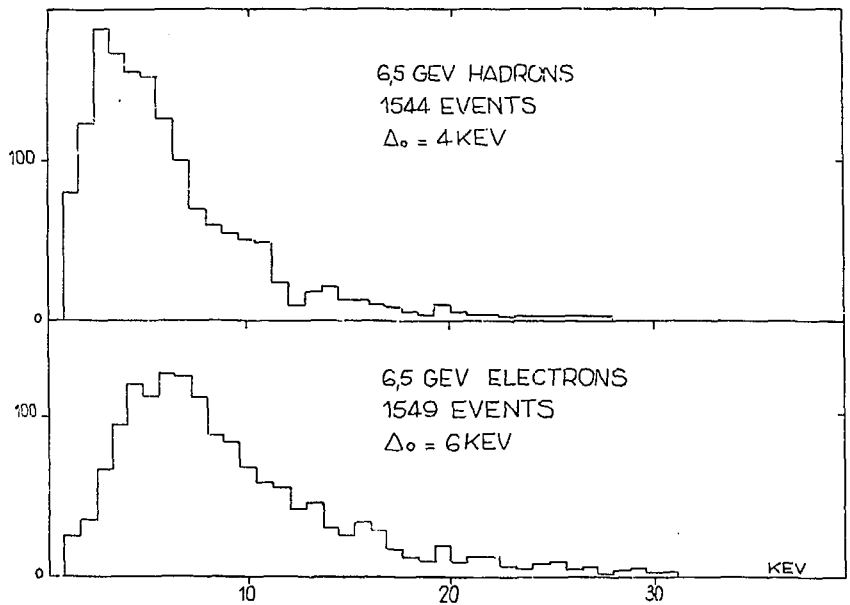

FIG.6 : dE/dx DISTRIBUTIONS AT 6.5 GeV/c FOR HADRONS AND FOR ELECTRONS.

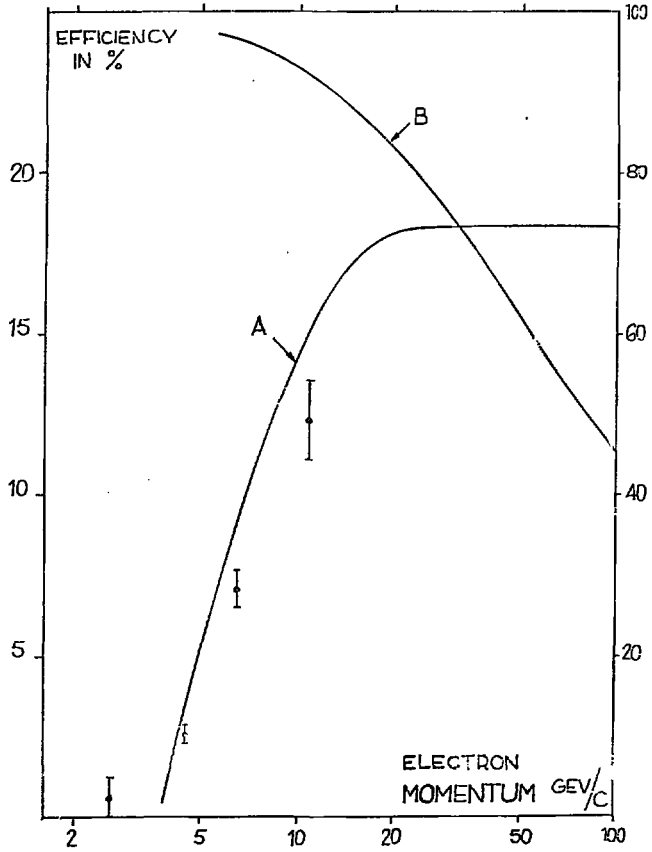

FIG.7 : SYNCHROTRON RADIATION. EXPECTED AND OBSERVED EFFICIENCIES AS A FUNCTION OF THE ELECTRON MOMENTUM.

CURVE (A) WITH THE LEFT HAND SIDE SCALE CORRESPONDS TO ρ = 50 M AND $\Delta\theta$ = 5.5 MRAD.
CURVE (B) (RIGHT HAND SIDE SCALE) IS OBTAINED WITH A FIELD OF 20 KGAUSS OVER 2 M.